A seismoelectric inverse problem with well-log data and borehole-confined acquisition

Aimé Fournier, Charles-Henri Clerget, Pawan Bharadwaj, MIT Earth Resources Laboratory and Ioan Alexandru Merciu, Gjertrud Skår, Equinor*

SUMMARY

One of the formation properties that most can impact drilling risk is pore-fluid pressure. While the literature abounds with analyses, computation and laboratory experiments, and case studies purportedly providing the remote estimation of pressure, none has yet lead to a technology that is confidently adopted in general drilling situations, or even in well-defined specific situations. It is a consequence of physics that direct measurement of pressure can be performed only by sensors in contact with the medium; whereas indirect, remote estimation may be enabled by the effect of pressure on mechanical or electromagnetic fields propagating through the bulk to recording receivers. Technology has not been confidently adopted mainly due to large uncertainties of how measurable formation properties relate measurable fields to pressure. To advance this situation, in our research program we propose to combine:

- a new, hypothetical downhole tool using acoustic sources with geophones and electric receivers along the drill string;
- a new LWD system, firing drill-string sources designed to concentrate acoustic energy in a spatially compact locus many 10s of meters ahead of the bit; and
- a new real-time inversion problem comprising estimation of zonation i.e., formation layer interfaces, jointly from concurrent drilling-operation parameters and seismoelectric gradient-response signals, plus estimation of uniform acoustic and electric properties within depth intervals.

The aim of this program, ultimately to be conjoined with petrophysical and geomechanical modeling based on zonation and interval properties, is to estimate pore pressure many 10s of meters ahead of the drill bit. This abstract presents a preliminary outline of the tool and system, a formal sensitivity analysis of the inversion computation procedure with respect to the properties being estimated, and numerical simulations of just the seismoelectric aspect of its overall operation, in a field populated by properties from actual well logs.

INTRODUCTION

Uncertain estimation of pore-fluid pressure p presents multiple drilling risks, chiefly being drilling-fluid loss or kicks. Physical considerations imply that p can be measured directly only by a sensor in contact with the medium, such as a calibrated strain gauge. It is possible to remotely estimate p due to its effect on mechanical or electromagnetic waves propagating through the bulk to recording receivers, using formulations such as effective stress tensor, as reviewed by e.g., Zhang (2011). None of the analyses, computation and laboratory experiments, and case studies that purportedly provides the remote estimation of pressure has yet lead to a technology that is confidently adopted in general drilling situations, or even in well-defined specific situations. The lack of confidence is mainly due to large uncertainties of how measurable formation properties connect measurable waves to pressure, including:

- prior uncertainties e.g., of reservoir-model boundary conditions, history (how rivers, glaciers, lakes and other mechanisms have transported the deposits in uneven patterns) and other parameters;
- other model uncertainties e.g., petrophysical parametrizations, geological deposits, impurities, zonation (formation layer interfaces), depth assignment etc.;
- local-measurement uncertainties e.g., geophone or antenna sensitivities; and
- remote-measurement uncertainties e.g., of interpreting reflector locations, orientations and contrasts.

The following sections present a preliminary design of the tool and system, a formal sensitivity analysis of the inversion computation procedure with respect to the properties being estimated, and numerical simulations of just the seismoelectric gradient-response aspect of its overall operation, in a field populated by properties from actual well logs.

METHOD

LWD system

The real-time prediction of p from borehole data goes back at least to Dutta et al. (2001, and refs. therein), who proposed to predict overpressure hazards using: borehole data; wireline vertical seismic profiles (VSPs, noting that VSPs incur rig downtime); and drill-bit seismic. Khaitan et al. (2013) showed how VSP could reduce p uncertainty and inform drilling and casing decision making, but Ranjan et al. (2017, Fig. 1) laid out how much uncertainty increases with range ahead of the bit. Figure 1 illustrates the sequential Bayesian estimation-while-drilling concept that we have developed internally since 2016. Other researchers (e.g., Paglia et al., 2019) recently presented similar elements, how estimates of p anomaly become more precise, through sequentially applying Bayes' rule to the current prior and LWD information, to create a new posterior that will become the next prior. Our approach will significantly augment such estimates by performing active seismoelectric inversion in real time. The BHA* emits acoustic (more generally, elastic, poroelastic etc.) waves that are designed to concentrate in a small volume in order to maximize conversion to electric signal as explained below. By minimizing the

* Tool illustration is not intended for practice, just a suggestive image from https://drilling-manual.blogspot.com/2017/11/bha-types.html

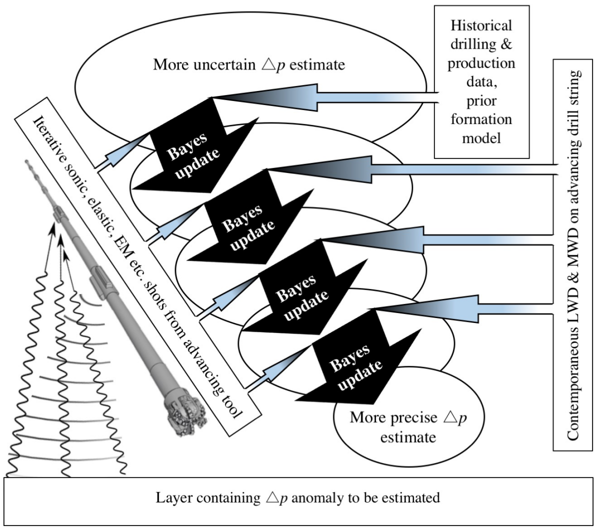

Figure 1: Sequential Bayesian estimation while drilling (black arrows). The right call-outs feed in prior and contemporaneous information relative to the current drill position, and the left call-out feeds active formation measurements ahead and around the advancing drill bit. Ellipses represent uncertainty of the p anomaly in the lower box ahead of the drill.

measurement-simulation misfit, properties such as conductivity and zonation —the position of surfaces of discontinuity (or regions of large gradient) can be inferred.

Forward problem

The acoustic wave in the bulk, with isotropic stress P and displacement rate $\mathbf{V}$, is governed by a differential equation

$$\left(\frac{\partial}{\partial t}+\begin{pmatrix}0 & \rho c^2\nabla\cdot\\ \rho^{-1}\nabla & 0\end{pmatrix}\right)\begin{pmatrix}P\\ \mathbf{V}\end{pmatrix}=\begin{pmatrix}0\\ \mathbf{F}_{\mathrm{s}}\end{pmatrix}, \qquad (1)$$

where $c(\mathbf{x})$ and $\rho(\mathbf{x})$ are the acoustic-wavespeed and mass-density functions of the medium and $\mathbf{F}_{\mathrm{s}}$ represents external sources. Empirically, the fluid pressure and flow velocity $p = BP$ and $\mathbf{v} = -\lambda\nabla p$ are obtained from the bulk ones using Skempton's coefficient B and Darcy's Law, where λ is the ratio of mobility to porosity. An electrical diffuse layer present between the fluid and skeleton implies a current $(q/\lambda)\mathbf{v}$, the proportionality factor q/λ defined for convenience below. This induces a balancing electrostatic current $-\sigma\nabla\psi$, conductivity multiplying electric-potential gradient. Putting all these together, the divergence of Ampère's Law requires

$$\nabla\cdot(\sigma\nabla\psi+q\nabla(BP))=0. \qquad (2)$$

Equation 2 is an elliptic partial differential equation to be solved for ψ given the parameter functions $B(\mathbf{x})$, $q(\mathbf{x})$ and $\sigma(\mathbf{x})$, field $P(t,\mathbf{x})$ from (1), and boundary conditions on insulating or conducting boundaries (e.g., Grobbe et al., 2019). The formal structure of (2) is

$$\mathscr{L}[\sigma]\psi=-\mathscr{L}[q]p, \qquad (3)$$

where $\mathscr{L}[r]=\nabla\cdot r\nabla$ is an elliptic partial differential operator if $r(\mathbf{x})>0$ for all $\mathbf{x}$ in the domain.

SENSITIVITY ANALYSIS

The sensitivity of $\psi(t,\mathbf{x}'')$ to $\sigma(\mathbf{x})$ would be determined by Fréchet differentiation of $(\mathscr{L}[\sigma]u)(\mathbf{x}')$ for arbitrary $u(\mathbf{x}'')$,

$$\begin{aligned}((\mathscr{L}[\sigma+\varepsilon]-\mathscr{L}[\sigma])u)(\mathbf{x}') &= \left\langle\delta(\cdot-\mathbf{x}'),\nabla\cdot\varepsilon\nabla u\right\rangle\\ &= -\left\langle\nabla\delta(\cdot-\mathbf{x}')\cdot\nabla u,\varepsilon\right\rangle\\ \Leftrightarrow\qquad \frac{\partial\mathscr{L}}{\partial\sigma(\mathbf{x})} &= -\nabla\delta(\mathbf{x}-\cdot)\cdot\nabla,\end{aligned}$$

an operator with a very sparse numerical discretization, requiring no storage. Holding p and q as fixed functions, the variation of (3) would determine a 2-point sensitivity field $\partial\psi(t,\mathbf{x}'')/\partial\sigma(\mathbf{x})$ as the solution of

$$\mathscr{L}[\sigma]\frac{\partial\psi}{\partial\sigma}=-\frac{\partial\mathscr{L}}{\partial\sigma}\psi \qquad (4)$$

(e.g., Fichtner and Trampert, 2011, eq. 15), except implying large storage that should be avoided. It is sufficient to study the squared error norm between simulation and measurement,

$$\Phi=\frac{1}{2}\|\psi-\psi_{\mathrm{meas}}\|^2 \qquad (5)$$

with Fréchet derivative

$$\frac{\partial\Phi}{\partial\sigma}=\left\langle\psi-\psi_{\mathrm{meas}},\frac{\partial\psi}{\partial\sigma}\right\rangle=-\left\langle\chi,\frac{\partial\mathscr{L}}{\partial\sigma}\psi\right\rangle \qquad (6)$$

if the adjoint field χ is determined as follows. Applying (4) to (6) yields $\left\langle\chi,\mathscr{L}[\sigma]\frac{\partial\psi}{\partial\sigma}\right\rangle=\left\langle\mathscr{L}[\sigma]\chi,\frac{\partial\psi}{\partial\sigma}\right\rangle$, since $\mathscr{L}[\sigma]$ is self-adjoint. So by (6), χ must satisfy

$$\mathscr{L}[\sigma]\chi=\psi-\psi_{\mathrm{meas}} \qquad (7)$$

(e.g., Fichtner and Trampert, 2011, eq. 23). Aghasi and Miller (2012) calculated sensitivities of other equations like (2).

Approximate Hessian kernels

Using (4), let the linearized forward modeling operation that maps the conductivity perturbations $\triangle\sigma(\mathbf{x})$ to the electric-potential perturbation $\triangle\psi(t,\mathbf{x}'')$ at the receivers be denoted

$$(\mathscr{F}\triangle\sigma)(t,\mathbf{x}'')=\triangle\psi(t,\mathbf{x}'')=\left\langle\frac{\partial\psi(t,\mathbf{x}'')}{\partial\sigma},\triangle\sigma\right\rangle$$

(e.g., Fichtner and Trampert, 2011, eq. 30). For sensitivity analysis, we estimate the approximate Hessian kernel

$$\left\langle\mathscr{F}\delta(\cdot-\mathbf{x}'),\mathscr{F}\delta(\cdot-\mathbf{x}'')\right\rangle \qquad (8)$$

(cf., Fichtner and Trampert, 2011, eq. 34). Figure 2 visualizes (8) with our proposed acquisition geometry comprising an acoustic source at $\mathbf{x}_{\mathrm{s}}=(40,25)$ m and 8 collinear receivers on a drill string, drilling a medium with uniform $\sigma(\mathbf{x})=10$ S m^{-1} and $c(\mathbf{x})=3000$ m s^{-1}. Recalling the use of the Hessian in classical Newton's iterations, these plots show that the influence of any local update $\triangle\sigma(\mathbf{x}'')$ upon the reduction that $\triangle\sigma(\mathbf{x}')$ induces in (5) is sensitive mostly just to radial differences $\|\mathbf{x}'-\mathbf{x}_{\mathrm{s}}\|-\|\mathbf{x}''-\mathbf{x}_{\mathrm{s}}\|$, not to directional differences between $\mathbf{x}'-\mathbf{x}_{\mathrm{s}}$ and $\mathbf{x}''-\mathbf{x}_{\mathrm{s}}$ (in distinction from purely acoustic Hessians e.g., Fichtner and Trampert, 2011, fig. 2). Thus, σ contrasts closer to $\mathbf{x}_{\mathrm{s}}$ will be better resolved than farther ones.

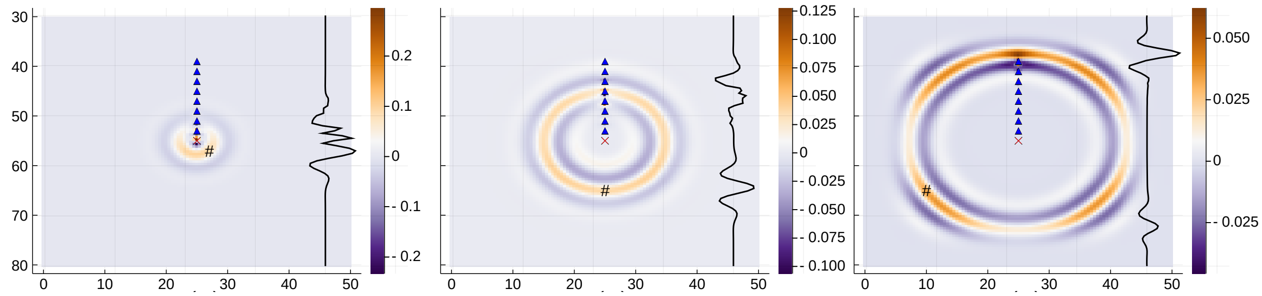

Figure 2: Approximate Hessian kernels (eq. 8, colors) vs depth x_1' (ordinate, m) and x_2' (abscissa, m) for 3 reference locations $\mathbf{x}''$ (# markers). Triangle and cross markers show the receivers and source locations. Black curves indicate x_2'-integrated kernels.

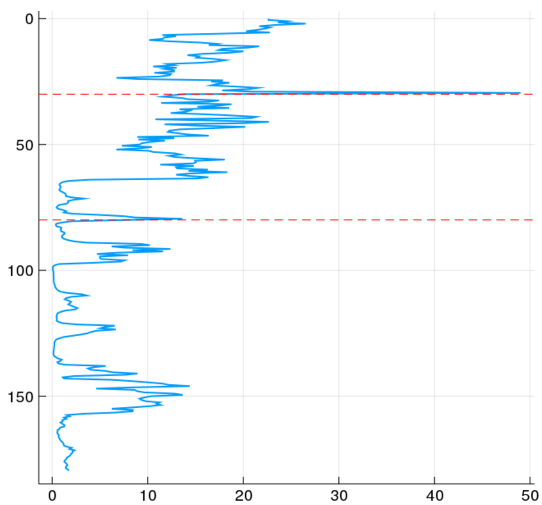

Figure 3: Measured σ (abscissa) vs depth x_1 (ordinate) from a single well, sampled each 15 cm for about 180 m. The reference x_1 has been subtracted and $1/\sigma$ has been scaled to have unit mean. Dashed lines show the extracted 30 m $\leq x_1 \leq$ 80 m.

Well log data

To avoid most of the aforementioned directional ambiguity, we assume the medium is layered in x_1, and independent of x_2,

$$\sigma(\mathbf{x}) = \sigma(x_1), \tag{9}$$

leaving only up-down ambiguity, as illustrated by the black curves of Figure 2. Data shown in Figure 3 come from actual logs from an offshore deviated well, and are used below.

NUMERICAL SIMULATIONS

In this section, we use Figure 3 as a true model, and the simple acquisition geometry described above. The inverse problem defined by minimizing (5) is ill-posed due to the limited acquisition geometry, and some regularization must be used (e.g., Willoughby, 1979). First, we require the inversion to return only layered solutions of the form (9). Then, we add an explicit regularizing term $R(\sigma)$ to (5), to promote specific structure in σ. The most classical choice would be Tikhonov regularization,

$$R(\sigma) \to \|\mathscr{C}^{-1/2}(\sigma - \sigma_0)\|_2^2, \tag{10}$$

which can be interpreted in a Bayesian view as enforcing a Gaussian prior distribution with mean $\sigma_0(\mathbf{x})$ and covariance operator $\mathscr{C}$. However, this view actually militates against (10) for the Figure-3 true model. Indeed, inspecting the σ histogram over all of Figure 3, the Gaussian assumption is inappropriate; the distribution exhibits significant skewness (1.03) and kurtosis (1.68). From a physical view, since conductivity in nature must be positive, but often is very small, the distribution is asymmetric, and displays a relatively long tail of large values. Thus it is more appropriate to assume as prior that σ follows a log-normal distribution,

$$R(\sigma) = \|\mathscr{C}^{-1/2}(\ln\sigma - \ln\sigma_0)\|_2^2. \tag{11}$$

The optimal choice for $\mathscr{C}$ is to take the covariance operator of the distribution of $\ln\sigma$. Practically, we can estimate $\mathscr{C}$ using the empirical variogram of the Figure-3 data, fitting an exponential model (see Armstrong, 1998). We take $\ln\sigma_0$ to be the average value of $\ln\sigma$ over the domain.

The inversion is run by stacking $\psi_{\text{meas}}(t,\cdot)$ measurements taken at 30 values of t following the emission of a spherical wave by the source. The pressure field (not shown) over the employed t essentially resembles a wavelet propagating outward along the $\|\mathbf{x}-\mathbf{x}_s\| - ct$ front, and is uniformly sampled over t. The limiting factor in the sampling of the measurement is the computational burden of the forward modeling (eqs. 1, 3) and gradient codes (7), as it is proportional to the number of t samples.

The inversion result is displayed in Figure 4 (left). The trend of the distribution is very well captured away from the domain boundaries. In particular, the sharp decrease of σ ahead of the tool (which is of primary interest to us for drilling monitoring and risk-assessment purposes) is very well reconstructed.

DISCUSSION

The limitations of the inversion near the domain boundaries (especially above the receivers) illustrates the up-down ambiguity discussed above. Three main approaches can be considered to lift this uncertainty:

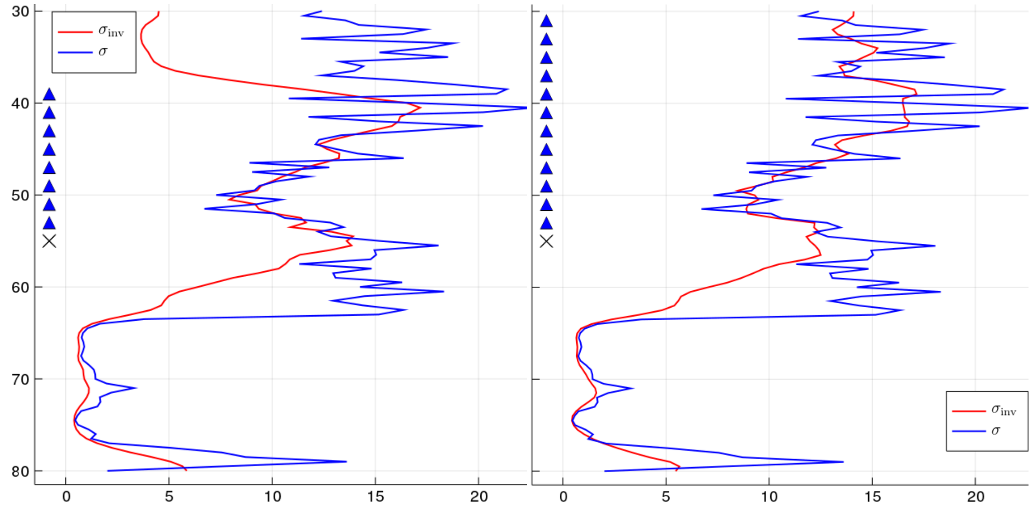

Figure 4: Conductivity σ, true values (blue) and results from inversion (red) for 8 (left) or 12 (right) receivers as shown by triangle markers.

- adding direct measurements behind the bit (e.g, if a LWD resistivity tool is used) in the sequential Bayesian estimation approach described by Figure 1;
- using acoustic source arrays to concentrate seismoelectric conversion above and below independently; or
- increasing the number of electrodes above the tool to measure a larger part of the domain with direct transmission.

The results of the third approach are shown in Figure 4 (right). As expected, the reconstruction in the upper domain is now very good. Interestingly, this also improves the inversion ahead of the tool, consistent with the fact that, by reducing the uncertainty behind the bit, we can better allocate data misfit to the model ahead of it.

CONCLUSIONS

There are many causes of uncertainty in estimating pore-fluid pressure. Estimation some 10s of meters ahead of the drill bit,

- using
  - sources and receivers confined to the borehole, and
  - other borehole measurements behind the bit,
- but
  - without VSP, cross-well seismic or any other signals transmitted through the medium, and
  - with low confidence in the resolution of reservoir structures and other confounding or uncertain factors in the prior models,

is challenging in the extreme. Our collaboration responds to this challenge in three primary ways.

- Focus on a new kind of measurement ahead of the bit, seismoelectric conversion, that although relatively weak and subject to complications, is known to be sensitive to contrasts of conductivity and other formation properties.
- First use seismoelectric conversion to identify zonation (boundaries of sharp contrasts between smoothly varying properties), then estimate uniform property values within the identified zones.
- Accept that the proliferation of uncertainties prevents very accurate estimates, but enough information may be obtained to assess risk and make other decisions.

In this abstract we have presented the preliminary design for a measurement system to accomplish sufficiently informative pore-pressure estimation for decision making. We analyzed the simplified electrostatic model coupled to charges in pore-fluid flow, how sensitive it is to conductivity perturbations. Based on this analysis (and other practical considerations), we chose to model conductivity as vertical layers. With limited but realistic acquisition geometry, we obtained acceptable inversion results compared to actual well-log conductivity.

ACKNOWLEDGMENTS

We gratefully acknowledge the data shared by Equinor under Contract 4503452749, which data are confidential. The data and results are provided on an “as is” basis and may contain errors and omissions. The authors provide no warranties, expressed or implied, either relating to the content or to the relevance of this document, disclaim any liability for errors and defects associated with the data to the maximum extent permitted by law, and shall not be liable for any direct or indirect losses as a result of use of the information.

REFERENCES

Aghasi, A., and E. L. Miller, 2012, Sensitivity calculations for Poisson's equation via the adjoint field method: IEEE Geoscience and Remote Sensing Letters, **9**, 237–241.

Armstrong, M., 1998, Basic linear geostatistics: Springer.

Dutta, N. C., W. H. Borland, W. Scott Leaney, R. Meehan, and W. Les Nutt, 2001, Pore pressure ahead of the bit: An integrated approach, *in* Pressure Regimes in Sedimentary Basins and Their Prediction: American Association of Petroleum Geologists.

Fichtner, A., and J. Trampert, 2011, Hessian kernels of seismic data functionals based upon adjoint techniques: Geophysical Journal International, **185**, 775–798.

Grobbe, N., A. Fournier, and L. Demanet, 2019, Seismoelectric conversion: U.S. Patent Application 16/361,073, International Patent Application PCT/US2019/023456.

Khaitan, M., P. Tyagi, A. Dwivedi, and D. Srinivas, 2013, Successful prediction of depth and velocity using look-ahead vertical seismic profile inversion to reduce drilling uncertainties: Presented at the 10th Biennial International Conference and Exposition on the theme "Changing Landscapes in Geophysical Innovations".

Paglia, J., J. Eidsvik, A. Grøver, and A. E. Lothe, 2019, Statistical modeling for real-time pore pressure prediction from predrill analysis and well logs: Geophysics, **84**.

Ranjan, P., M. Khaitan, S. Chandrasekhar, and B. Kumar, 2017, Vsp lookahead of the bit information: Considerations and accuracy analysis: Presented at the AAPG Asia Pacific Region Geosciences Technology Workshop, Oil and Gas Resources of India: Exploration and Production Opportunities and Challenges.

Willoughby, R., 1979, Solutions of ill-posed problems (A.N. Tikhonov and V.Y. Arsenin): SIAM Review, **21**, 266–267.

Zhang, J., 2011, Pore pressure prediction from well logs: Methods, modifications, and new approaches: Earth-Science Reviews.